










# Observational constraints and dynamical analysis of Kaniadakis horizon-entropy cosmology

A. Hernández-Almada <sup>1</sup> \*, Genly Leon <sup>2,3</sup>, Juan Magaña <sup>4</sup>, Miguel A. García-Aspeitia <sup>5</sup>,  
V. Motta <sup>6</sup>, Emmanuel N. Saridakis <sup>7,8,9</sup>, Kuralay Yesmakhanova <sup>9,10</sup>, Alfredo D. Millano <sup>2</sup>

<sup>1</sup>Facultad de Ingeniería, Universidad Autónoma de Querétaro, Centro Universitario Cerro de las Campanas, 76010, Santiago de Querétaro, México,

<sup>2</sup>Departamento de Matemáticas, Universidad Católica del Norte, Avda. Angamos 0610, Casilla 1280 Antofagasta, Chile,

<sup>3</sup>Institute of Systems Science, Durban University of Technology, PO Box 1334, Durban 4000, South Africa

<sup>4</sup>Instituto de Astrofísica & Centro de Astro-Ingeniería, Pontificia Universidad Católica de Chile, Av. Vicuña Mackenna, 4860, Santiago, Chile,

<sup>5</sup>Depto. de Física y Matemáticas, Universidad Iberoamericana Ciudad de México, Prolongación Paseo

de la Reforma 880, México D. F. 01219, México

<sup>6</sup>Instituto de Física y Astronomía, Facultad de Ciencias, Universidad de Valparaíso,

Avda. Gran Bretaña 1111, Valparaíso, Chile,

<sup>7</sup>Institute for Astronomy, Astrophysics, Space Applications and Remote Sensing, National Observatory of Athens, Lofos Nymfon, 11852 Athens, Greece,

<sup>8</sup>CAS Key Laboratory for Researches in Galaxies and Cosmology, Department of Astronomy,

University of Science and Technology of China, Hefei, Anhui 230026, P.R. China,

<sup>9</sup>Ratbay Myrzakulov Eurasian International Centre for Theoretical Physics, Nur-Sultan 010009, Kazakhstan,

<sup>10</sup>Ratbay Myrzakulov Eurasian International Centre for Theoretical Physics, Eurasian National University, Nur-Sultan Astana 010008, Kazakhstan.

21 March 2022

## ABSTRACT

We study the scenario of Kanadiakis horizon entropy cosmology which arises from the application of the gravity-thermodynamics conjecture using the Kaniadakis modified entropy. The resulting modified Friedmann equations contain extra terms that constitute an effective dark energy sector. We use data from Cosmic chronometers, Supernova Type Ia, HII galaxies, Strong lensing systems, and Baryon acoustic oscillations observations and we apply a Bayesian Markov Chain Monte Carlo analysis to construct the likelihood contours for the model parameters. We find that the Kaniadakis parameter is constrained around 0, namely, around the value where the standard Bekenstein-Hawking is recovered. Concerning the normalized Hubble parameter, we find  $h = 0.708^{+0.012}_{-0.011}$ , a result that is independently verified by applying the  $H_0(z)$  diagnostic and, thus, we conclude that the scenario at hand can alleviate the  $H_0$  tension problem. Regarding the transition redshift, the reconstruction of the cosmographic parameters gives  $z_T = 0.715^{+0.042}_{-0.041}$ . Furthermore, we apply the AICc, BIC and DIC information criteria and we find that in most datasets the scenario is statistical equivalent to  $\Lambda$ CDM one. Moreover, we examine the Big Bang Nucleosynthesis (BBN) and we show that the scenario satisfies the corresponding requirements. Additionally, we perform a phase-space analysis, and we show that the Universe past attractor is the matter-dominated epoch, while at late times the Universe results in the dark-energy-dominated solution. Finally, we show that Kanadiakis horizon entropy cosmology accepts heteroclinic sequences, but it cannot exhibit bounce and turnaround solutions.

**Key words:** theory, dark energy, cosmological parameters.

## 1 INTRODUCTION

Cosmology is one of the most exciting adventures in the human endeavour: the understanding of the origin, evolution and future of our Universe by combining the physics at micro- and macro-scales in a joint framework. In particular, the Universe acceleration is one of the most important puzzles. Discovered by the Supernovae team, through type Ia supernovae (SNIa, Riess et al. 1998), it is also confirmed by the acoustic peaks of the Cosmic Microwave Background Radiation (CMB, Spergel et al. 2003), and recently tested with large-scale structure measurements (Nadathur et al. 2020). Tackling the Universe acceleration is indeed a complicated issue due to the at-

tractive nature of gravity in the General Relativity (GR) framework. The first approach on its explanation is through the addition of the cosmological constant (CC, Carroll 2001). Thus, using the continuity equation and assuming a constant energy density ( $\dot{\rho} = 0$ ), it is possible to conclude that the equation of state (EoS) is  $w = -1$ , which is in concordance with what is expected for a fluid that accelerates the Universe. Another main characteristic is that the energy density of the CC must be subdominant in order to obtain a late and non-violent acceleration. From the Quantum Field Theory (QFT) viewpoint, the CC can be explained by the addition of quantum vacuum fluctuations (QVF) associated to the space-time. Therefore, the expansion of space-time implies an increase of QVF, maintaining a constant energy density. However, when we calculate the energy density of the QVF, the result is in complete disagreement with the

\* Contact e-mail: [ahalmada@uaq.mx](mailto:ahalmada@uaq.mx)

observed one (see Zel'dovich et al. 1968; Weinberg 1989), this is the so-called *fine tuning problem* (Addazi et al. 2021). In addition to the cosmological constant problem, a  $4.2\sigma$  tension in the current Hubble parameter value ( $H_0$ ) measured by Supernova  $H_0$  for the Equation of State (SH0ES) collaboration (Riess et al. 2021) and the one obtained by Planck collaboration under the  $\Lambda$ -Cold Dark Matter ( $\Lambda$ CDM) scenario (Aghanim et al. 2020) has been recently observed.

The above mentioned problems that afflicts the understanding of the CC in this framework has driven the community to propose other approaches like scalar fields, dynamical dark energy, viscous fluids, Chaplygin gas (Hernández-Almada, A. et al. 2019) or modifications to GR such as unimodular gravity (García-Aspeitia et al. 2019; García-Aspeitia et al. 2021), Einstein-Gauss-Bonnet (García-Aspeitia & Hernández-Almada 2021), Brane Worlds (García-Aspeitia et al. 2018), among others (see Saridakis et al. 2021; Motta et al. 2021, for a compilation of the mentioned previous models). Despite the fact that we can have numerous models and scenarios describing the late time acceleration, at the end of the day the detailed confrontation with observations, alongside theoretical consistency, will be the main method for their validation.

One interesting alternative to investigate the dynamics of the Universe is the gravity-thermodynamics approach (Jacobson 1995; Padmanabhan 2005, 2010). This takes advantage of the first law of thermodynamics and the standard Bekenstein-Hawking entropy-area relation for black holes, which applied to the apparent cosmological horizon leads to the Friedmann equations (Frolov & Kofman 2003; Cai & Kim 2005; Akbar & Cai 2007; Cai & Cao 2007). Hence, the application of this conjecture with various alternative entropy relations leads to modified Friedmann equations whose additional terms can source the cosmic acceleration (Cai & Cao 2007; Akbar & Cai 2006; Paranjape et al. 2006; Sheykhi et al. 2007; Jamil et al. 2010b; Cai & Ohta 2010; Wang et al. 2010; Jamil et al. 2010a; Sheykhi 2010b,a; Gim et al. 2014; Fan & Lu 2015; Lympers & Saridakis 2018; Sheykhi 2018; Saridakis 2020).

One interesting class of extended entropies arises through generalizations for the Boltzmann-Gibbs statistics. In particular, one modifies the classical entropy of a system given by  $S = -k_B \sum_i p_i \ln p_i$ , where  $p_i$  is the probability of a system to be within a microstate, through non-extensive analysis resulting into the Tsallis entropy (Tsallis 1988; Lyra & Tsallis 1998), through quantum-gravitational considerations resulting into Barrow entropy (Barrow 2020), or through relativistic extensions resulting into Kaniadakis entropy (Kaniadakis 2002, 2005). Hence, the application of the gravity-thermodynamics conjecture using the above modified horizon entropy gives rise to modified cosmological scenarios. In Lympers & Saridakis (2018) this was performed in the framework of Tsallis entropy, in Saridakis (2020); Saridakis & Basilakos (2021); Leon et al. (2021); Barrow et al. (2021a) applied it for the Barrow entropy case, and recently (Lympers et al. 2021) use it in the Kaniadakis entropy frame.

In the present work, we investigate Kaniadakis horizon entropy cosmology by confronting it to observational data from Cosmic Chronometers, Supernovae Type I (SNIa), HII galaxies, strong lensing systems (SLS), and baryon acoustic oscillations (BAO) observations. Additionally, we perform a complete dynamical system analysis in order to extract information of the local and global features of the cosmological evolution.

The outline of the paper is as follows: Sec. 2 introduces the framework of the Kaniadakis cosmology. In Sec. 3 we infer the cosmological parameter under the Kaniadakis model using five observational datasets mentioned above. The section 4 presents a stability analysis around the equilibrium points of the dynamical system under

the Kaniadakis cosmology. Finally, we discuss and summarize our results in Section 5. From now on we use natural units in which  $\hbar = k_B = c = 1$ .

## 2 KANIADAKIS HORIZON ENTROPY COSMOLOGY

In this section we present the scenario of Kaniadakis horizon entropy cosmology (Lympers et al. 2021), namely the modified Friedmann equations arising from the application of the gravity-thermodynamics conjecture using the extended Kaniadakis entropy.

Kaniadakis entropy is an one-parameter generalization of the classical entropy, given as  $S_K = -k_B \sum_i n_i \ln_{\{K\}} n_i$  (Kaniadakis 2002, 2005), with  $k_B$  the Boltzmann constant and where  $\ln_{\{K\}} x = (x^K - x^{-K})/2K$ . In such a framework the dimensionless parameter  $-1 < K < 1$  quantifies the relativistic deviations from standard statistical mechanics, and the latter is recovered in the limit  $K \rightarrow 0$ . Kaniadakis entropy can be expressed as (Abreu et al. 2016, 2018; Abreu & Ananias Neto 2021)

$$S_K = -k_B \sum_{i=1}^W \frac{P_i^{1+K} - P_i^{1-K}}{2K}, \quad (1)$$

with  $P_i$  the probability of a specific microstate and  $W$  the total configuration number. When we apply it in the black-hole framework, we obtain (Drepanou et al. 2021; Moradpour et al. 2020; Lympers et al. 2021)

$$S_K = \frac{1}{K} \sinh(KS_{BH}), \quad (2)$$

where

$$S_{BH} = \frac{1}{4G} A, \quad (3)$$

is the usual Bekenstein-Hawking entropy, with  $A$  the horizon area and  $G$  is the gravitational constant. Hence, in the limit  $K \rightarrow 0$  we recover Bekenstein-Hawking entropy.

Let us now apply the gravity-thermodynamics conjecture using Kaniadakis entropy. We consider a flat homogeneous and isotropic Friedmann-Robertson-Walker (FRW) metric of the form

$$ds^2 = -dt^2 + a^2(t) \left( dr^2 + r^2 d\Omega^2 \right), \quad (4)$$

where  $d\Omega^2 \equiv d\theta^2 + \sin^2 \theta d\varphi^2$  is the solid angle, and  $a(t)$  the scale factor. In this setup, the first law of thermodynamics is interpreted in terms of the heat/energy that flows through the apparent horizon of the Universe (Jacobson 1995; Padmanabhan 2005, 2010), which in the case of flat geometry is just (Bak & Rey 2000; Frolov & Kofman 2003; Cai & Kim 2005; Cai et al. 2009):

$$r_a = \frac{1}{H}, \quad (5)$$

where  $H = \dot{a}/a$  is the Hubble parameter (dots denote derivatives with respect to  $t$ ). Concerning the horizon temperature, this is given by the standard relation (Gibbons & Hawking 1977):

$$T = \frac{1}{2\pi r_a}. \quad (6)$$

Hence, the first law of thermodynamics is just  $-dE = TdS$ , where  $-dE = A(\rho_m + p_m)Hr_a dt$  is the energy flow through the horizon during a time interval  $dt$  in the case of a Universe filled with a matter perfect fluid with energy density  $\rho_m$  and pressure  $p_m$  (Cai & Kim 2005). Differentiating (2) we obtain

$$dS_K = \frac{8\pi}{4G} \cosh\left(K \frac{\pi}{GH^2}\right) r_a \dot{r}_a dt, \quad (7)$$

where we have used that  $A = 4\pi r_a^2 = 4\pi/H^2$ .

Inserting (3), (6), and (7) into the first law of thermodynamics, alongside with the relation  $\dot{r}_a = -\dot{H}/H^2$ , we acquire (Lympiris et al. 2021)

$$-4\pi G(\rho_m + p_m) = \dot{H} \cosh \left[ K \frac{\pi}{GH^2} \right]. \quad (8)$$

Thus, using the matter conservation equation

$$\dot{\rho}_m + 3H(\rho_m + p_m) = 0, \quad (9)$$

the integration of (8) leads to

$$\frac{8\pi G}{3} \rho_m = H^2 \cosh \left[ K \frac{\pi}{GH^2} \right] - \frac{K\pi}{G} \text{shi} \left[ K \frac{\pi}{GH^2} \right] - \frac{\Lambda}{3}, \quad (10)$$

with  $\Lambda$  the integration constant and  $\text{shi}(x) \equiv \int_0^x \sinh(x')/x' dx'$ , a mathematical odd function of  $x$  with no discontinuities.

The above equations (8) and (10) are the modified Friedmann equations in the scenario of Kaniadakis horizon entropy cosmology (Lympiris et al. 2021). As expected, in the limit  $K \rightarrow 0$  they turn into the standard ones. We can re-write them as

$$H^2 = \frac{8\pi G}{3} (\rho_m + \rho_{DE}), \quad (11)$$

$$\dot{H} = -4\pi G(\rho_m + \rho_{DE} + p_m + p_{DE}), \quad (12)$$

where we have introduced an effective dark-energy sector, with energy density and pressure respectively of the form

$$\rho_{DE} = \frac{3}{8\pi G} \left\{ \frac{\Lambda}{3} + H^2 \left[ 1 - \cosh \left( \frac{\pi K}{GH^2} \right) \right] + \frac{\pi K}{G} \text{shi} \left( \frac{\pi K}{GH^2} \right) \right\}, \quad (13)$$

$$p_{DE} = -\frac{1}{8\pi G} \left\{ \Lambda + (3H^2 + 2\dot{H}) \left[ 1 - \cosh \left( \frac{\pi K}{GH^2} \right) \right] + \frac{3\pi K}{G} \text{shi} \left( \frac{\pi K}{GH^2} \right) \right\}. \quad (14)$$

Therefore, the EoS parameter for the dark energy sector is

$$w_{DE} = -1 - 2\dot{H} \left[ 1 - \cosh \left( \frac{\pi K}{GH^2} \right) \right] \times \left\{ \Lambda + 3H^2 \left[ 1 - \cosh \left( \frac{\pi K}{GH^2} \right) + \frac{3\pi K}{G} \text{shi} \left( \frac{\pi K}{GH^2} \right) \right] \right\}^{-1}. \quad (15)$$

In the general case, the cosmological equations are the two Friedmann equations (11) and (12), alongside the matter conservation equation (9). **For convenience we focus on the dust case, namely we consider  $p_m = 0$ .** It proves convenient to express the equations in terms of dimensionless variables. Introducing the density parameters

$$\Omega_\Lambda \equiv \frac{\Lambda}{3H^2}, \quad \Omega_m \equiv \frac{8\pi G \rho_m}{3H^2}, \quad (16)$$

the normalized Hubble function

$$E \equiv \frac{H}{H_0}, \quad (17)$$

with  $H_0$  the Hubble parameter at the present scale factor  $a_0$ , and defining the dimensionless parameter  $\beta$  as

$$\beta \equiv \frac{K\pi}{GH_0^2}, \quad (18)$$

then, the cosmological equations are expressed as

$$\Omega'_\Lambda(N) = 3\Omega_\Lambda \Omega_m \text{sech} \left( \frac{\beta}{E^2} \right), \quad (19)$$

$$\Omega'_m(N) = 3\Omega_m \left[ \Omega_m \text{sech} \left( \frac{\beta}{E^2} \right) - 1 \right], \quad (20)$$

$$E'(N) = -\frac{3}{2} E \Omega_m \text{sech} \left( \frac{\beta}{E^2} \right), \quad (21)$$

where primes denote derivatives with respect to the e-foldings number  $N = \ln(a/a_0)$  (and thus  $f' = \dot{f}/H$ ). Note that using the above variables, the first Friedmann equation (11) gives rise to the constraint

$$\beta \text{shi} \left( \frac{\beta}{E^2} \right) + E^2 \left[ -\cosh \left( \frac{\beta}{E^2} \right) + \Omega_\Lambda + \Omega_m \right] = 0, \quad (22)$$

which allows us to eliminate  $\Omega_\Lambda$  in terms of  $\Omega_m$  and  $E$ . Finally, note that for the effective dark energy density parameter, in the general case we have

$$\Omega_{DE} = 1 - \Omega_m = 1 + \beta \text{shi}(\beta) - \cosh(\beta) + \Omega_\Lambda. \quad (23)$$

Lastly, it proves convenient to introduce the deceleration parameter  $q(z)$ , and the cosmographic jerk parameter  $j(z)$ , which are defined as

$$q := -1 - \frac{E'}{E}, \quad (24)$$

$$j := q(2q + 1) - q', \quad (25)$$

where  $j = 1$  recovers the case of a cosmological constant.

In the scenario of Kaniadakis horizon entropy cosmology one may have the general integration constant  $\Lambda$ , which will play the role of an explicit cosmological constant, or one may set it to zero and thus require for the extra  $K$ -dependent terms to drive the Universe acceleration. Since the corresponding equation structure (which will be used later for the Bayesian statistical analysis and the dynamical system approach) is different in the two cases, we examine them separately in the following subsections.

## 2.1 Case I: $\Lambda \neq 0$

In the general case where  $\Lambda \neq 0$ , i.e.  $\Omega_\Lambda \neq 0$ , we use the constraint equation (22) to obtain the reduced dynamical system

$$\Omega'_m(N) = 3\Omega_m \left[ \Omega_m \text{sech} \left( \frac{\beta}{E^2} \right) - 1 \right], \quad (26)$$

$$E'(N) = -\frac{3}{2} E \Omega_m \text{sech} \left( \frac{\beta}{E^2} \right). \quad (27)$$

This is integrable, with

$$\Omega_m(E) = \cosh \left( \frac{\beta}{E^2} \right) + \frac{-\cosh(\beta) - \beta \text{shi} \left( \frac{\beta}{E^2} \right) + \beta \text{shi}(\beta) + \Omega_m^{(0)}}{E^2}, \quad (28)$$

$$\Omega_m(1) = \Omega_m^{(0)}, \quad (29)$$

and

$$E'(N) = -\frac{3}{2} E - \frac{3 \text{sech} \left( \frac{\beta}{E^2} \right) \left( -\cosh(\beta) - \beta \text{shi} \left( \frac{\beta}{E^2} \right) + \beta \text{shi}(\beta) + \Omega_m^{(0)} \right)}{2E}, \quad (30)$$

where  $\Omega_m(N=0) = \Omega_m^{(0)}$  and  $E(N=0) = 1$ .

The equation (30) is easily integrated to give

$$3N(E) = -\ln \left( 1 - \frac{\cosh(\beta) - E^2 \cosh \left( \frac{\beta}{E^2} \right) + \beta \text{shi} \left( \frac{\beta}{E^2} \right) - \beta \text{shi}(\beta)}{\Omega_m^{(0)}} \right), \quad (31)$$

introducing as dynamical variable the redshift  $e^N = a = (1+z)^{-1}$ , where  $z=0$  and  $a_0=1$  for current time, the previous equation leads to

$$(z+1)^3 = 1 - \frac{\left[ \cosh(\beta) - E^2 \cosh \left( \frac{\beta}{E^2} \right) + \beta \text{shi} \left( \frac{\beta}{E^2} \right) - \beta \text{shi}(\beta) \right]}{\Omega_m^{(0)}}. \quad (32)$$

Evaluating (23) at present time gives

$$\Omega_{DE}^{(0)} = 1 - \Omega_m^{(0)} = 1 + \beta \text{shi}(\beta) - \cosh(\beta) + \Omega_\Lambda^{(0)}, \quad (33)$$

and combining it with (32) we have

$$\Omega_m^{(0)}(z+1)^3 + \Omega_\Lambda^{(0)} = E^2 \cosh\left(\frac{\beta}{E^2}\right) - \beta \operatorname{sh}\left(\frac{\beta}{E^2}\right). \quad (34)$$

We mention here that in the general case where  $\Lambda \neq 0$  from the above we obtain the relation between  $\beta$ ,  $\Omega_m^{(0)}$  and  $\Omega_\Lambda^{(0)}$  as

$$\Omega_m^{(0)} = \cosh(\beta) - \beta \operatorname{sh}(\beta) - \Omega_\Lambda^{(0)}. \quad (35)$$

We expand (33), (34) up to third order around  $\beta = 0$ , resulting in

$$\Omega_m^{(0)} + \Omega_\Lambda^{(0)} = 1 - \frac{\beta^2}{2} + O(\beta^4), \quad (36)$$

and

$$\Omega_m^{(0)}(z+1)^3 + \Omega_\Lambda^{(0)} \approx E^2 - \frac{\beta^2}{2E^2} + O(\beta^4). \quad (37)$$

Hence, we obtain four roots:

$$E_{1,2} = \mp \frac{\sqrt{\Omega_m^{(0)}(z+1)^3 + \Omega_\Lambda^{(0)} - \sqrt{2\beta^2 + [\Omega_m^{(0)}(z+1)^3 + \Omega_\Lambda^{(0)}]^2}}}{\sqrt{2}}, \quad (38)$$

$$E_{3,4} = \mp \frac{\sqrt{\Omega_m^{(0)}(z+1)^3 + \Omega_\Lambda^{(0)} + \sqrt{2\beta^2 + [\Omega_m^{(0)}(z+1)^3 + \Omega_\Lambda^{(0)}]^2}}}{\sqrt{2}}. \quad (39)$$

Solutions  $E_1$  and  $E_2$  are complex, and  $E_3$  is negative. Thus, the only physical solution is  $E_4$ . In the following, instead of using the exact implicit formula for  $E$  given in (34), we will consider the approximation  $E_4$  in (39).

## 2.2 Case II: $\Lambda = 0$

In the case where an explicit cosmological constant is absent, namely  $\Lambda = 0$ , i.e.  $\Omega_\Lambda = 0$ , the general system (26), (27) reduces to

$$E'(N) = -\frac{3}{2}E + \frac{3\beta \operatorname{sech}\left(\frac{\beta}{E^2}\right) \operatorname{sh}\left(\frac{\beta}{E^2}\right)}{2E}. \quad (40)$$

The last equation is easily integrated to give

$$N(E) = -\frac{1}{3} \ln \left[ \frac{E^2 \cosh\left(\frac{\beta}{E^2}\right) - \beta \operatorname{sh}\left(\frac{\beta}{E^2}\right)}{\cosh(\beta) - \beta \operatorname{sh}(\beta)} \right], \quad (41)$$

which, using the redshift, implies

$$(z+1)^3 = \frac{E^2 \cosh\left(\frac{\beta}{E^2}\right) - \beta \operatorname{sh}\left(\frac{\beta}{E^2}\right)}{\cosh(\beta) - \beta \operatorname{sh}(\beta)}. \quad (42)$$

Hence, using

$$\Omega_m^{(0)} = \cosh(\beta) - \beta \operatorname{sh}(\beta), \quad (43)$$

as it arises from (35) for  $\Omega_\Lambda^{(0)} = 0$ , we obtain

$$\Omega_m^{(0)}(z+1)^3 = E^2 \cosh\left(\frac{\beta}{E^2}\right) - \beta \operatorname{sh}\left(\frac{\beta}{E^2}\right). \quad (44)$$

Expanding (44) up to third order around  $\beta = 0$ , we result to

$$\Omega_m^{(0)}(z+1)^3 \approx E^2 - \frac{\beta^2}{2E^2} + O(\beta^4), \quad (45)$$

and thus at present times gives  $\Omega_m^{(0)} = 1 - \frac{\beta^2}{2} + O(\beta^4)$ . Therefore, we obtain four roots:

$$E_{1,2} = \mp \frac{\sqrt{\Omega_m^{(0)}(z+1)^3 - \sqrt{2\beta^2 + \Omega_m^{(0)}(z+1)^6}}}{\sqrt{2}}, \quad (46)$$

$$E_{3,4} = \mp \frac{\sqrt{\Omega_m^{(0)}(z+1)^3 + \sqrt{2\beta^2 + \Omega_m^{(0)}(z+1)^6}}}{\sqrt{2}}. \quad (47)$$

Similarly to the previous case, roots  $E_1$  and  $E_2$  are complex while  $E_3$  is negative. Consequently, the only physical solution is  $E_4$  in (47).

## 3 OBSERVATIONAL CONSTRAINTS

In this section we confront the scenario of Kaniadakis horizon-entropy cosmology with observations. We are interested in extracting the bounds on the parameter phase-space  $\Theta = \{h, \Omega_m^{(0)}, \beta\}$  and  $\{h, \beta\}$ , particularly on the parameter  $\beta$ , which is related to the Kaniadakis basic parameter  $K$ . For convenience, we focus on the physically interested case of dust matter, namely we set  $w_m = 0$ .

### 3.1 Datasets and methodology

We will employ the most commonly used datasets.

- *Observational Hubble Data* (OHD). The sample contains 31 cosmological-independent measurements of the Hubble parameter in the redshift range  $0.07 < z < 1.965$  from passive elliptical galaxies, the so-called cosmic chronometers (Moresco et al. 2016).

- *Pantheon Supernova Type Ia sample* (SNIa). We use 1048 data points of the distance modulus,  $\mu(z)_{\text{SNIa}}$ , of high-redshift SNIa in the redshift range  $0.001 < z < 2.3$  (Scolnic et al. 2018).

- *HII galaxies* (HIIG). It contains a total of 181 data points of the distance modulus  $\mu_{\text{HIIG}}(z)$  estimated from the Balmer line luminosity-velocity dispersion relation for HII galaxies spanning the redshift region  $0.01 < z < 2.6$  (González-Morán et al. 2021).

- *Strong lensing systems* (SLS). We use the sample by Amante et al. (2020) which contains 143 strong lensing systems by elliptical galaxies with measurements of the redshift for the lens and the source, spectroscopic velocity dispersion and the Einstein radius. These quantities allow us to construct an observational distance ratio within the region  $0.5 \leq D^{\text{obs}} \leq 1$ .

- *Baryon acoustic oscillations* (BAO). We consider 6 correlated data points of the imprint of baryon acoustic oscillation in the size of the sound horizon in clustering and power spectrum of galaxies measured by Percival et al. (2010); Blake et al. (2011); Beutler et al. (2011) and collected by Giostri et al. (2012).

We would like to mention here that other cosmological observations could be included in the parameter estimation too, for instance the CMB data. To perform such analysis in a robust way, a full perturbation approach is needed in order to obtain the linear Einstein-Boltzmann equations. Nevertheless this is beyond the scope of the present work. An alternative approach would be to use the distance priors from Planck 2018 based on slight deviations from  $\Lambda$ CDM, such as the  $w$ CDM model (Chen et al. 2019). However, since this procedure could lead to biased constraints, in the following we prefer not to use the CMB dataset.

The inference of the cosmological parameters under Kaniadakis horizon entropy cosmology for both scenarios ( $\Lambda \neq 0$  and  $\Lambda = 0$ ) is performed by a Bayesian Markov Chain Monte Carlo (MCMC) approach and the emcee Python module (Foreman-Mackey et al.



2013). We set 3000 chains with 250 steps each, and consider uniform priors in the ranges:  $h : [0.2, 1]$ ,  $\Omega_m^{(0)} : [0, 1]$ ,  $\beta : [-\pi, \pi]$ . The burn-in phase is stopped up to obtain convergence according to the auto-correlation time criterion. Then, we build a Gaussian log-likelihood as the merit-of-function to minimize through the equation  $-2\ln(\mathcal{L}) \propto \chi^2$ , where  $\chi$  is the chi-square function given by

$$\chi_{\text{uncorr}}^2 = \sum_i^{N_{\text{dat}}} \left( \frac{\mathcal{D} - \mathcal{M}}{\sigma_{\mathcal{D}}} \right)^2, \quad (48)$$

for the samples OHD, HIIG, SLS because the measurements are considered to be uncorrelated.  $N_{\text{dat}}$  is the number of points of dataset  $\mathcal{D}$ ,  $\sigma_{\mathcal{D}}$  is the estimated uncertainty for each dataset, and  $\mathcal{M}$  represents the theoretical quantity of that observable **based on  $E_4$  presented in (39) and (47) for  $\Lambda \neq 0$  and  $\Lambda = 0$  models respectively**. As SNIa and BAO datasets contain correlated points, the figure of merit is built as

$$\chi_{\text{corr}}^2 = \Delta\vec{x} \cdot C^{-1} \cdot \Delta\vec{x}^T, \quad (49)$$

where  $\Delta\vec{x}$  is the difference between the observational and theoretical quantities, and  $C^{-1}$  is the covariance matrix. It is worth to mention that a nuisance parameter is presented in the SNIa data and it is convenient to marginalize over it to reduce the uncertainties. Thus, the figure of merit for SNIa data is

$$\chi_{\text{SNIa}}^2 = a + \ln\left(\frac{e}{2\pi}\right) - \frac{b^2}{e}, \quad (50)$$

where  $a$ ,  $b$ , and  $e$  are functions of  $\Delta\vec{x}$  and  $C^{-1}$ . For more details on these expressions see [Motta et al. \(2021\)](#).

Finally, we perform a joint analysis through the sum of the function-of-merits of each data sample, namely

$$\chi_{\text{Joint}}^2 = \chi_{\text{OHD}}^2 + \chi_{\text{SLS}}^2 + \chi_{\text{HIIG}}^2 + \chi_{\text{SNIa}}^2 + \chi_{\text{BAO}}^2, \quad (51)$$

where subscripts indicate the dataset under consideration.

### 3.2 Results

Performing the full confrontation of the scenario we construct the corresponding log-likelihood contours at 68% ( $1\sigma$ ) and 99.7% ( $3\sigma$ ) confidence level (CL), and we present them in Fig. 1 alongside the 1D posterior distribution. Moreover, in Table 1 we show the mean values and the uncertainties at  $1\sigma$  confidence level for the parameters  $h$ ,  $\Omega_m^{(0)}$  and  $\beta$  for both  $\Lambda \neq 0$  and  $\Lambda = 0$  cases.

As can be seen, the bounds estimated from each data sample are consistent among themselves, although the SLS dataset provides lower values for  $\Omega_m^{(0)}$ . The joint constraints  $h = 0.708_{-0.011}^{+0.012}$  ( $h = 0.715_{-0.012}^{+0.012}$ ) for the case  $\Lambda \neq 0$  ( $\Lambda = 0$ ), are consistent at  $2.67\sigma$  ( $3\sigma$ ) with the one estimated from the CMB anisotropies ([Aghanim et al. 2020](#)) and at  $1.74\sigma$  ( $1.36\sigma$ ) with the one from SH0ES ([Riess et al. 2019](#)). Hence, the scenario of Kaniadakis horizon entropy cosmology can offer an alleviation to the  $H_0$  tension, providing a value in between its local measurements, and its indirect estimation from the early stages of the Universe.

Concerning Kaniadakis parameter, we find that, when  $\Lambda \neq 0$ , the combination of the data samples constrains  $\beta = -0.011_{-0.507}^{+0.515}$ , namely  $\beta$  is constrained around 0 as expected, the value in which Kaniadakis entropy becomes the standard Bekenstein-Hawking one. However, when  $\Lambda = 0$ , the joint constraint yields  $\beta = 1.161_{-0.013}^{+0.013}$ , which is expected, as we mentioned above, because in the absence of an explicit cosmological constant one needs a significant deviation from standard cosmology to describe the Universe acceleration. Finally, note that due to equation (43) that holds in the  $\Lambda = 0$  case, we

acquire a correlation between  $\Omega_m^{(0)}$  and the Kaniadakis parameter  $\beta$  in the lower panel of Fig. 1.

Let us make a comment on the predicted entropy today, since this is possible to be calculated through Eq. (2). According to our model, and imposing for the horizon area of our Universe its present value, we arrive at the value  $S_K \sim 1.44 \times 10^{99} \text{ m}^2 \text{ Kg s}^{-2} \text{ K}^{-1}$  (for  $\Lambda \neq 0$ ) and  $S_K \sim 3.15 \times 10^{99} \text{ m}^2 \text{ Kg s}^{-2} \text{ K}^{-1}$  (for  $\Lambda = 0$ ). In comparison, for the standard Bekenstein-Hawking entropy, we have  $S_{BH} \sim 2.83 \times 10^{99} \text{ m}^2 \text{ Kg s}^{-2} \text{ K}^{-1}$  ( $\Lambda \neq 0$ ) and  $S_{BH} \sim 2.79 \times 10^{99} \text{ m}^2 \text{ Kg s}^{-2} \text{ K}^{-1}$  ( $\Lambda = 0$ ). Therefore, the corresponding ratio is  $S_K/S_{BH} \simeq 0.5$  for  $\Lambda \neq 0$  and  $S_K/S_{BH} \simeq 1.12$  for  $\Lambda = 0$ , which implies a small difference between Kaniadakis and Bekenstein-Hawking entropies.

Due to the competitive qualities of the fits obtained from both scenarios, it would be interesting to statistically compare them with the concordance  $\Lambda$ CDM cosmology. In order to achieve this, we apply the standard criteria, namely the Akaike information criterion corrected for small samples (AICc, [Akaike 1974](#); [Sugiura 1978](#); [Hurvich & Tsai 1989](#)) and the Bayesian information criterion (BIC, [Schwarz 1978](#)), since  $\Lambda \neq 0$  model contains one extra free parameter over  $\Lambda$ CDM. The AICc and BIC are defined as  $\text{AICc} = \chi_{\text{min}}^2 + 2k + (2k^2 + 2k)/(N - k - 1)$  and  $\text{BIC} = \chi_{\text{min}}^2 + k \ln(N)$  respectively, where  $\chi_{\text{min}}^2$  is the minimum of the  $\chi^2$  function,  $N$  is the size of the dataset and  $k$  is the number of free parameters. Following the rules described in [Hernández-Almada et al. \(2022\)](#), we find that  $\Lambda = 0$  model and  $\Lambda$ CDM are statistically equivalent based on AICc ( $\Delta\text{AICc} < 4$ ), when the sample are treated separately, but show a strong evidence against ( $6 < \text{BIC} < 10$ ) the scenario when the joint analysis is applied. On the other hand, although AICc suggests that  $\Lambda \neq 0$  model and  $\Lambda$ CDM are statistically equivalent in the joint analysis, BIC indicates that there is a strong evidence against the candidate model. Additionally, for the two models we find that the  $\Lambda = 0$  case is preferred by separate datasets, while the  $\Lambda \neq 0$  case is statistically preferred for the combined data analysis.

For completeness, we additionally calculate the Deviance information criterion (DIC, [Spiegelhalter et al. 2002](#); [Kunz et al. 2006](#); [Liddle 2007](#)). This is defined as  $\text{DIC} = D(\bar{\theta}) + 2p_D$ , where  $D(\bar{\theta}) = \chi^2(\bar{\theta})$  is the Bayesian deviation,  $p_D = \bar{D}(\theta) - D(\bar{\theta})$  is the Bayesian complexity, which represents the number of effective degrees of freedom, and  $\bar{\theta}$  is the mean value of the parameters. The advantage of DIC is its use of the full log-likelihood sample instead of only the maximum log-likelihood (or minimum  $\chi^2$ ) as AICc and BIC do. Based on the Jeffreys scale ([Jeffreys 1961](#)), for  $\Delta\text{DIC} < 2$  both models are statistical equivalent. In contrast,  $2 < \Delta\text{DIC} < 6$  suggests a moderate tension between models, being the one with lower value of DIC the best one, and  $\Delta\text{DIC} > 10$  implies a strong tension between the two models. We find that the  $\Lambda \neq 0$  case and  $\Lambda$ CDM scenario are statistical equivalent for BAO, they have a moderate tension for OHD and SLS, and a strong tension for HIIG and SNIa. On the other hand, the  $\Lambda \neq 0$  case and  $\Lambda$ CDM are statistical equivalent for OHD, BAO, HIIG, and SNIa. In summary, we confirm the results obtained for the Joint analysis by AICc and BIC for both  $\Lambda \neq 0$  and  $\Lambda = 0$  models. It is worth to mention that when a posterior distribution presents a bimodal shape or is asymmetric for a parameter,  $p_D$  yields negative values and thus DIC may not be a good criterion. This situation is mainly presented for  $\beta$  in the  $\Lambda \neq 0$  case in separate datasets.

As a next step, we use the constraints from the joint analysis to reconstruct the three cosmographic parameters, namely the Hubble,  $H(z)$ , the deceleration,  $q(z)$ , and jerk,  $j(z)$ , parameters according to (24), (25). The cosmic evolution of parameters is shown in Fig. 2. Thus, we report the current values of  $q_0 = -0.610_{-0.035}^{+0.028}$  ( $-0.708_{-0.016}^{+0.016}$ ) for the deceleration parameter, and  $j_0 = 1.041_{-0.036}^{+0.051}$

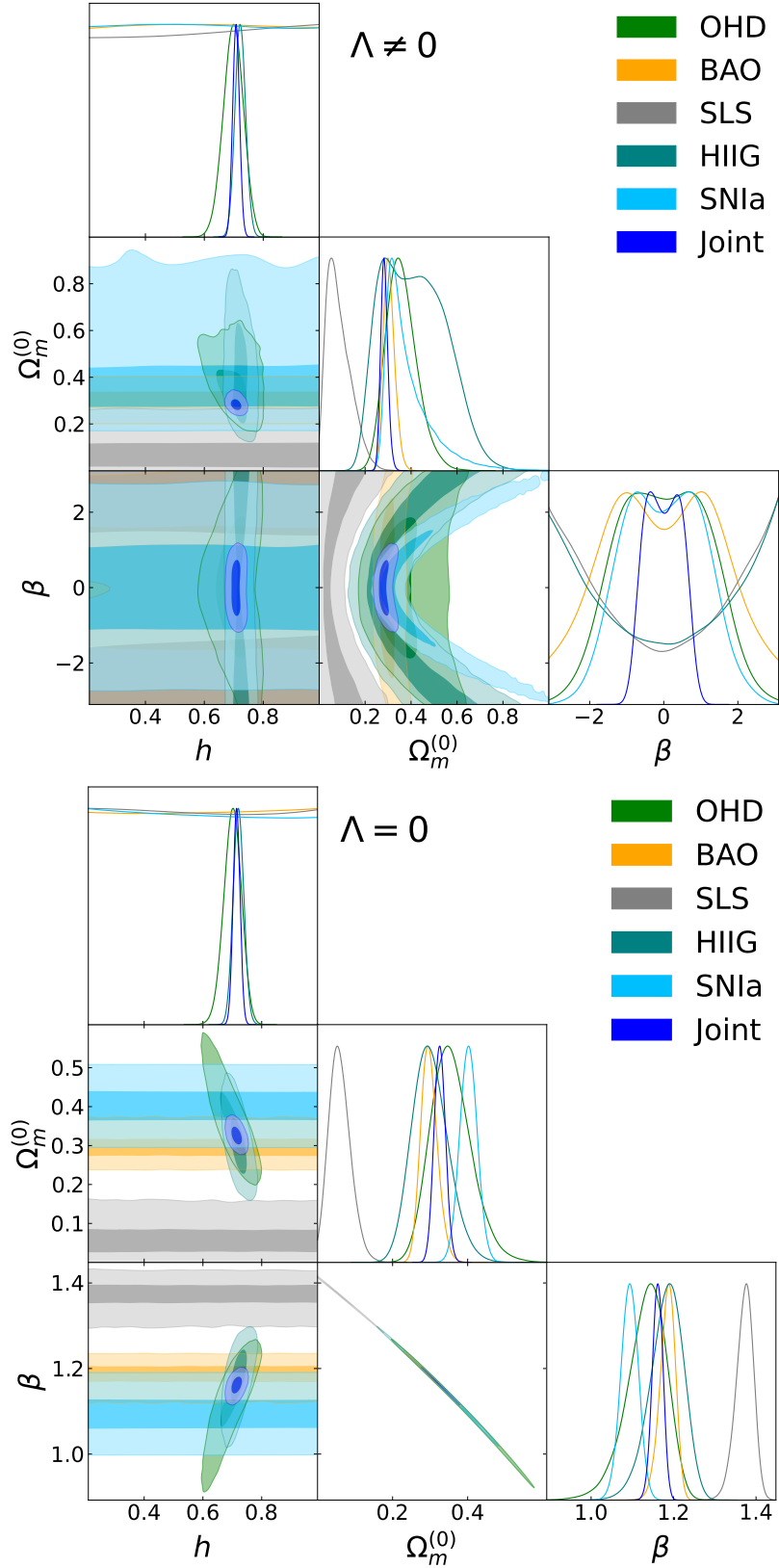


**Figure 1.** Two-dimensional log-likelihood contours at 68% and 99.7% confidence level (CL), alongside the corresponding 1D posterior distribution of the free parameters, in Kaniadakis horizon entropy cosmology, for  $\Lambda \neq 0$  (upper panel) and  $\Lambda = 0$  (lower panel). We use the various datasets described in the text, as well as the joint analysis.

Sample	$\chi^2_{\min}$	$h$	$\Omega_m^{(0)}$	$\beta$	$\Delta\text{AICc}$	$\Delta\text{BIC}$	$\Delta\text{DIC}$
Case $\Lambda \neq 0$							
OHD	19.25	$0.699^{+0.033}_{-0.034}$	$0.354^{+0.072}_{-0.061}$	$-0.004^{+1.259}_{-1.255}$	7.6	8.2	-4.5
BAO	2.91	$0.599^{+0.272}_{-0.270}$	$0.302^{+0.027}_{-0.023}$	$-0.016^{+1.596}_{-1.594}$	14.1	1.9	0.2
SLS	216.52	$0.608^{+0.268}_{-0.277}$	$0.077^{+0.064}_{-0.042}$	$-0.006^{+2.550}_{-2.526}$	5.5	8.3	-5.2
HIIG	452.96	$0.722^{+0.018}_{-0.018}$	$0.408^{+0.151}_{-0.137}$	$0.043^{+2.510}_{-2.562}$	19.3	22.3	-19.6
SNIa	1042.99	$0.598^{+0.273}_{-0.270}$	$0.359^{+0.126}_{-0.055}$	$0.009^{+1.108}_{-1.124}$	9.0	14.0	-14.6
Joint	1743.48	$0.708^{+0.012}_{-0.011}$	$0.283^{+0.016}_{-0.015}$	$-0.011^{+0.517}_{-0.507}$	2.9	8.1	0.5
Case $\Lambda = 0$							
OHD	14.56	$0.701^{+0.029}_{-0.030}$	$0.353^{+0.057}_{-0.050}$	$1.138^{+0.043}_{-0.051}$	0.5	0.0	0.0
BAO	2.33	$0.602^{+0.272}_{-0.273}$	$0.297^{+0.023}_{-0.021}$	$1.186^{+0.017}_{-0.020}$	3.6	-0.4	-0.3
SLS	212.86	$0.596^{+0.276}_{-0.270}$	$0.057^{+0.031}_{-0.027}$	$1.373^{+0.020}_{-0.023}$	-0.2	-0.3	0.0
HIIG	435.64	$0.721^{+0.018}_{-0.018}$	$0.298^{+0.050}_{-0.045}$	$1.185^{+0.038}_{-0.043}$	-0.1	-0.2	-0.1
SNIa	1036.48	$0.596^{+0.275}_{-0.271}$	$0.402^{+0.023}_{-0.023}$	$1.093^{+0.021}_{-0.021}$	0.5	0.5	0.5
Joint	1753.03	$0.715^{+0.012}_{-0.012}$	$0.326^{+0.015}_{-0.015}$	$1.161^{+0.013}_{-0.013}$	10.4	10.4	10.4

**Table 1.** Best-fit values and their 68% CL uncertainties for Kaniadakis horizon entropy cosmology with  $\Lambda \neq 0$  (upper panel) and  $\Lambda = 0$  (lower panel) employing the data sets: OHD (31 data points), BAO (6 data points), SLS (143 data points), HIIG (181 data points), SNIa (1048 data points) and the joint analysis of them.

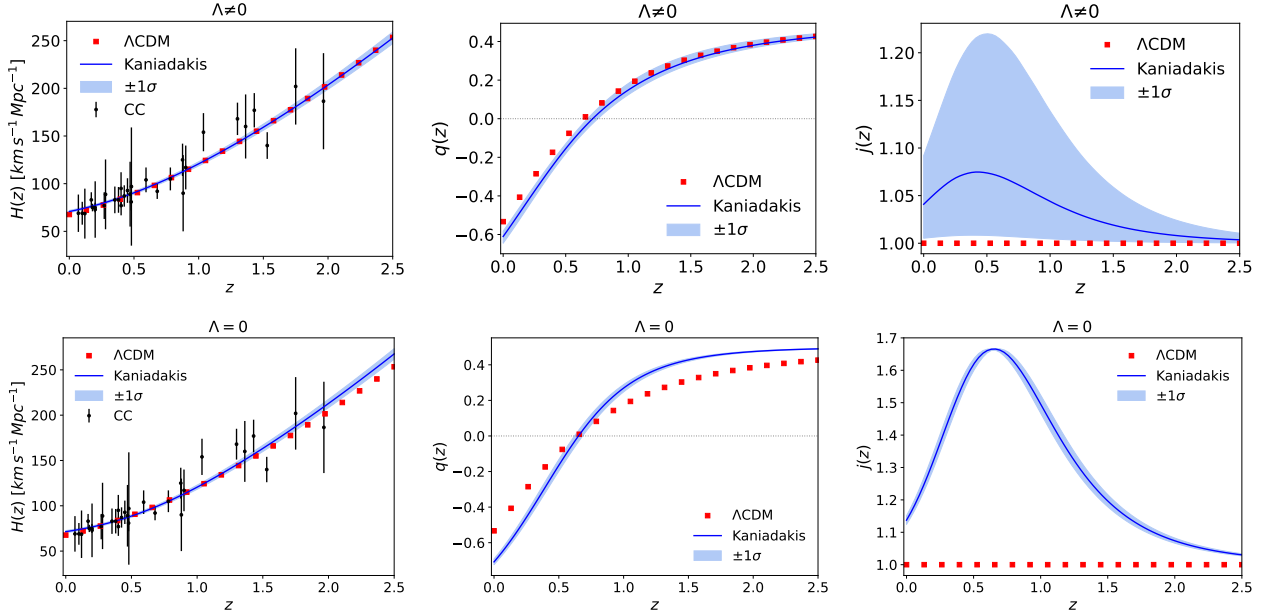


**Figure 2.** Upper panel, left to right: reconstruction of the  $H(z)$ ,  $q(z)$ , and  $j(z)$ , in Kaniadakis horizon entropy cosmology with  $\Lambda \neq 0$ . Lower panel: same as before for the case  $\Lambda = 0$ . We have used the bound obtained from the joint analysis, and the shaded regions denote the uncertainties at  $1\sigma$ . For completeness, the red square-points represent the results of  $\Lambda\text{CDM}$  cosmology with  $h = 0.6766$  and  $\Omega_m^{(0)} = 0.3111$  (Aghanim et al. 2020).

$(1.137^{+0.014}_{-0.013})$  for the jerk parameter for the  $\Lambda \neq 0$  ( $\Lambda = 0$ ) scenario. Furthermore, the transition redshift between the deceleration and the acceleration stages is estimated to be  $z_T = 0.715^{+0.042}_{-0.041}$  ( $0.652^{+0.032}_{-0.031}$ ), which is in agreement with the one obtained by  $\Lambda\text{CDM}$  as shown in Fig. 2. Note that the jerk parameter evolution reveals the dynamical equation of state of the effective dark energy.

Finally, to investigate in more detail the Hubble tension, we apply a new diagnostic, called  $\mathbb{H}0(z)$  diagnostic, defined by (Krishnan et al. 2021)

$$\mathbb{H}0(z) = \frac{H(z)}{E_{\Lambda\text{CDM}}(z)}, \quad (52)$$

where  $H(z)$  is the Hubble function evolution in a given cosmological

scenario alternative to  $\Lambda\text{CDM}$ , and  $E_{\Lambda\text{CDM}}(z)$  is the dimensionless Hubble parameter of  $\Lambda\text{CDM}$  paradigm. This diagnostic measures a possible deviation of  $H_0$  from its  $\Lambda\text{CDM}$  value. Concerning a flat  $\Lambda\text{CDM}$ , a non-constant path of  $\mathbb{H}0(z)$  within error bars suggests a modification of the Planck- $\Lambda\text{CDM}$  scenario. In Fig. 3 we depict the obtained results.

As we observe, there is an agreement within  $1\sigma$  between flat- $\Lambda\text{CDM}$  cosmology and Kaniadakis cosmology for  $z \gtrsim 0.7$  in the  $\Lambda \neq 0$  case, and for  $0.7 \lesssim z \lesssim 1.3$  in the  $\Lambda = 0$  case. Additionally, it is interesting that the current value  $\mathbb{H}0(z=0)$  for both models are consistent with the one obtained by SH0ES (Riess et al. 2019), and that the  $\Lambda \neq 0$  model has a trend to the Planck value in the past (Aghanim et al. 2020). This is another verification that the scenario

of Kaniadakis horizon entropy cosmology may offer an alleviation to the  $H_0$  tension. Nevertheless, to further investigate whether both Kaniadakis models can alleviate the Hubble tension, a parameter estimation using the linear perturbation equations together with CMB data should be performed.

We close this section by investigating one important process in every cosmological scenario: the Big Bang Nucleosynthesis (BBN), since the production of light elements in the early Universe can be affected in non-standard cosmologies (Pospelov & Pradler 2010; Barrow et al. 2021b). Considering that the freeze-out of the light elements occurs when the weak interaction rates are lower than  $H(z)$ , a simple test to guarantee that the BBN is not spoiled is to require that the deviation  $\delta H(z)$  with respect to the standard Hubble expansion rate at the BBN epoch should be small. Although in the Friedmann equations mentioned above we have not included a radiation component, this can be added and we can perform the analysis by expanding  $E_4$  around  $\beta = 0$  in Eq. (39) (resp. Eq. (47)) and neglecting the fourth order error terms, resulting to

$$E(z) = \begin{cases} \underbrace{\sqrt{\Omega_m^{(0)}(z+1)^3 + \Omega_\Lambda^{(0)}}}_{\text{value from } \Lambda\text{CDM}} + \underbrace{\frac{\beta^2}{4} \left[ \Omega_m^{(0)}(z+1)^3 + \Omega_\Lambda^{(0)} \right]^{-3/2}}_{\text{correction}}, & \Lambda \neq 0 \\ \underbrace{\sqrt{\Omega_m^{(0)}(z+1)^3}}_{\text{value from } \Lambda\text{CDM}} + \underbrace{\frac{\beta^2}{4} \left[ \Omega_m^{(0)} \right]^{-3/2} (z+1)^{-1/2}}_{\text{correction}}, & \Lambda = 0 \end{cases} \quad (53)$$

Hence, we can study both Kaniadakis models ( $\Lambda \neq 0$  and  $\Lambda = 0$ ) at  $z \sim 10^{10}$  (approximately BBN era). We find that for  $\Lambda \neq 0$ , the model is consistent with the Big Bang Nucleosynthesis (BBN) constraints, since the correction term at  $z \sim 10^{10}$  is of the order of  $\sim 10^{-49}$ , dominating the standard cosmology and not producing significant effects in the formation of light elements. In the case  $\Lambda = 0$ , the correction is larger, and calculations at  $z \sim 10^{10}$  are of the order  $\sim 10^{-5}$ . However, such corrections are still subdominant, allowing the production of light elements. A further analysis could be performed following Capozziello et al. (2017); Barrow et al. (2021b); Asimakis et al. (2021).

#### 4 DYNAMICAL SYSTEM AND STABILITY ANALYSIS

In this section we perform a full dynamical system analysis in order to investigate the global dynamics of cosmological scenarios, and obtain information on the Universe evolution independently of the initial conditions. In the dynamical system formulation, one starts from local analysis of the differential equation  $\mathbf{x}'(\tau) = \mathbf{X}(\mathbf{x})$ , where  $\mathbf{x}$  is the state vector, and  $\tau$  a convenient time variable, near an equilibrium point  $\mathbf{x} = \bar{\mathbf{x}}$ , and progressively extends the investigated regions of the phase and of the parameter space. Assuming that the vector field  $\mathbf{X}(\mathbf{x})$  has continuous partial derivatives, the process of determining the local behavior is based on the linear approximation of the vector field  $\mathbf{X}(\mathbf{x}) \approx \mathbf{DX}(\bar{\mathbf{x}})(\mathbf{x} - \bar{\mathbf{x}})$  where  $\mathbf{DX}(\bar{\mathbf{x}})$  is the Jacobian of the vector field at the equilibrium point  $\bar{\mathbf{x}}$ , which is referred to as the *linearization of the dynamical equations at the equilibrium point*. In this neighborhood we acquire the system  $\mathbf{x}'(\tau) = \mathbf{DX}(\bar{\mathbf{x}})(\mathbf{x} - \bar{\mathbf{x}})$ . Each of the equilibrium points can be classified according to the real parts of the eigenvalues of  $\mathbf{DX}(\bar{\mathbf{x}})$  (if none of these are zero). Thus, this approach provides a general description of the phase space of all possible solutions of the system, their equilibrium points and stability, as well as the asymptotic solutions (Wainwright & Ellis 1997; Ferreira & Joyce 1997; Copeland et al. 1998; Perko 2000; Coley 2003; Copeland et al. 2006; Chen et al. 2009; Cotsakis & Kittou 2013; Giambo & Miritzis 2010; Papagiannopoulos et al. 2022). If

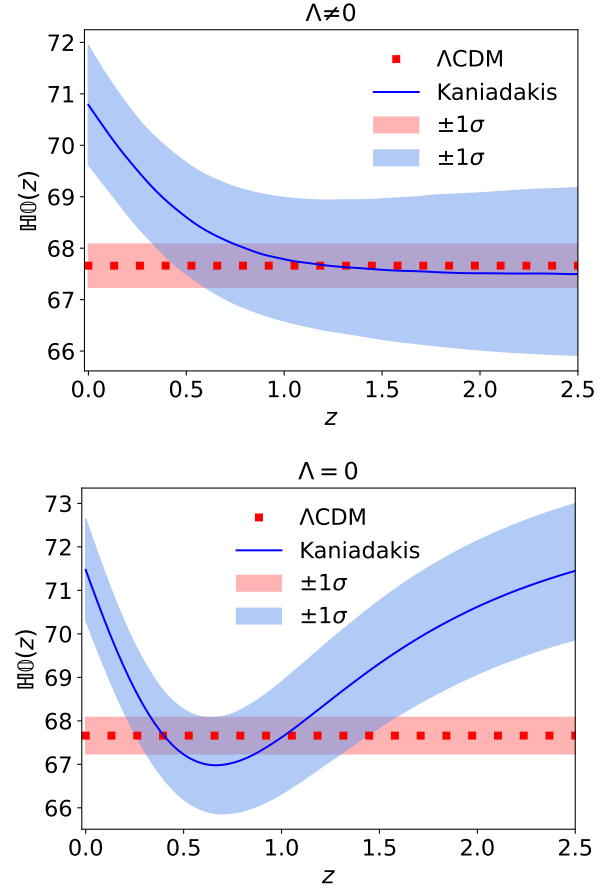


**Figure 3.** The  $H_0(z)$  diagnostic for Kaniadakis horizon entropy cosmology with  $\Lambda \neq 0$  (upper panel) and  $\Lambda = 0$  (lower panel). We have used the bound obtained from the joint analysis, and the shaded regions denote the uncertainties at  $1\sigma$ . For completeness, the red square-points represent the results of  $\Lambda\text{CDM}$  cosmology with  $h = 0.6766$  and  $\Omega_m^{(0)} = 0.3111$  (Aghanim et al. 2020).

some real parts of the eigenvalues are zero, the equilibrium point is nonhyperbolic, and the analysis through linearization fails. Then, we use numerical tools for the analysis.

In the following subsections we perform the global dynamical system analysis for the two cases, namely  $\Lambda \neq 0$  and  $\Lambda = 0$ .

##### 4.1 Case I: $\Lambda \neq 0$

Defining the dimensionless variables  $\theta, T$  as

$$\theta = \arctan \left( 1 - \frac{8\pi G \rho_{DE}}{3H^2} \right), \quad \theta \in \left[ -\frac{\pi}{2}, \frac{\pi}{2} \right], \quad T = \frac{H_0}{H + H_0}, \quad (54)$$

with

$$\Omega_m := \frac{8\pi G \rho_m}{3H^2} = \tan(\theta), \quad (55)$$

then equation (10) becomes

$$\frac{\Lambda}{3H_0^2} = \frac{(1-T)^2 \left\{ \cosh \left[ \frac{T^2 \beta}{(1-T)^2} \right] - \tan(\theta) \right\}}{T^2} - \beta \text{shi} \left[ \frac{T^2 \beta}{(1-T)^2} \right]. \quad (56)$$



Label	$\theta$	$T$	Existence	Stability
$dS_+$	$2\pi c_1$	arbitrary	$c_1 \in \mathbb{Z}$	stable
$dS_+^{(0)}$	$2\pi c_1$	0	$c_1 \in \mathbb{Z}$	stable
$dS_+^{(1)}$	$2\pi c_1$	1	$c_1 \in \mathbb{Z}$	stable
$dS_-$	$\pi(1+2c_1)$	arbitrary	$c_1 \in \mathbb{Z}$	stable
$dS_-^{(0)}$	$\pi(1+2c_1)$	0	$c_1 \in \mathbb{Z}$	stable
$dS_-^{(1)}$	$\pi(1+2c_1)$	1	$c_1 \in \mathbb{Z}$	stable
$M_-^{(0)}$	$2\pi c_1 - \frac{3\pi}{4}$	0	$c_1 \in \mathbb{Z}$	unstable
$M_+^{(0)}$	$2\pi c_1 + \frac{\pi}{4}$	0	$c_1 \in \mathbb{Z}$	unstable
$M_-^{(1)}$	$2\pi c_1 - \frac{3\pi}{4}$	1	$c_1 \in \mathbb{Z}, \beta = 0$	saddle
$M_+^{(1)}$	$2\pi c_1 + \frac{\pi}{4}$	1	$c_1 \in \mathbb{Z}, \beta = 0$	saddle

**Table 2.** The equilibrium points of the dynamical system (58) and (59) of Kaniadakis horizon entropy cosmology with  $\Lambda \neq 0$ . We use  $dS$  to denote the de Sitter, dark-energy dominated solutions, and  $M$  to denote the matter-dominated ones.

It proves convenient to introduce the new time derivative as

$$f' \equiv \frac{df}{d\tau} = \frac{\cosh\left(\frac{\pi K}{GH^2}\right)}{H} \dot{f}. \quad (57)$$

Therefore, we finally extract the dynamical system

$$\theta'(\tau) = 3 \sin(\theta) \left\{ \sin(\theta) - \cos(\theta) \cosh\left[\frac{T^2 \beta}{(1-T)^2}\right] \right\}, \quad (58)$$

$$T'(\tau) = \frac{3}{2}(1-T)T \tan(\theta). \quad (59)$$

Note that this system diverges at  $T = 1$  and at  $\theta = \pm\pi/2$ .

Lastly, the deceleration parameter (24) is written as

$$q := -1 - \frac{\dot{H}}{H^2} = -1 + \frac{3}{2} \tan(\theta) \operatorname{sech}\left[\frac{\beta T^2}{(1-T)^2}\right]. \quad (60)$$

Note that, for an expanding universe ( $H > 0$ ), we have that  $T \in [0, 1]$ , while  $\theta$  is a periodic coordinate with period  $\pi$ , and thus we can set  $\theta \in [-\pi/2, \pi/2]$  (modulo a periodic shift  $c\pi$ ,  $c \in \mathbb{Z}$ ). Moreover, the physical condition  $0 \leq \Omega_m \leq 1$  implies that the region of physical interest is  $\theta \in [0, \pi/4]$  (modulo a periodic shift  $c\pi$ ,  $c \in \mathbb{Z}$ ). The non-physical region  $\Omega_m > 1$  is  $\theta \in (\pi/4, \pi/2]$  (modulo a periodic shift  $c\pi$ ,  $c \in \mathbb{Z}$ ). Hence, we have obtained a global phase-space formulation. For the representation of the flow of (58) and (59), we integrate in the variables  $T, \theta$  and project in a compact set using the ‘‘cylinder-adapted’’ coordinates

$$\mathbf{S} : \begin{cases} x = \cos(\theta), \\ y = \sin(\theta), \\ z = T, \end{cases} \quad (61)$$

with  $0 \leq T \leq 1, \theta \in [-\pi, \pi]$ , with inverse  $\theta = \arctan(y/x)$ , and  $T = z$ . Thus, the region of physical interest is  $\theta \in [0, \pi/4]$ , modulo a periodic shift  $c\pi$ ,  $c \in \mathbb{Z}$ .

We proceed by extracting the equilibrium points and characterizing their stability. There are two equivalent hyperbolic equilibrium points  $M_{\pm}$  for which  $q = 1/2$ , i.e. they are associated with matter domination, and two equilibrium points  $dS_{\pm}$  corresponding to dark-energy dominated de-Sitter solutions for which  $q = -1$ . The equilibrium points of the dynamical system (58) and (59) of Kaniadakis horizon entropy cosmology with  $\Lambda \neq 0$  are presented in Table 2. In Fig. 4 we display an unwrapped solution space of the system (58) and (59) (upper panel), and the projection over the cylinder  $\mathbf{S}$ , defined in Cartesian coordinates  $(x, y, z)$  by (61), for the best fit value  $\beta = -0.011$  obtained through the observational analysis. For the points that are non-hyperbolic, their stability is analyzed numerically. The two dashed lines, indicated by  $dS_-$  (blue) and  $dS_+$  (red),

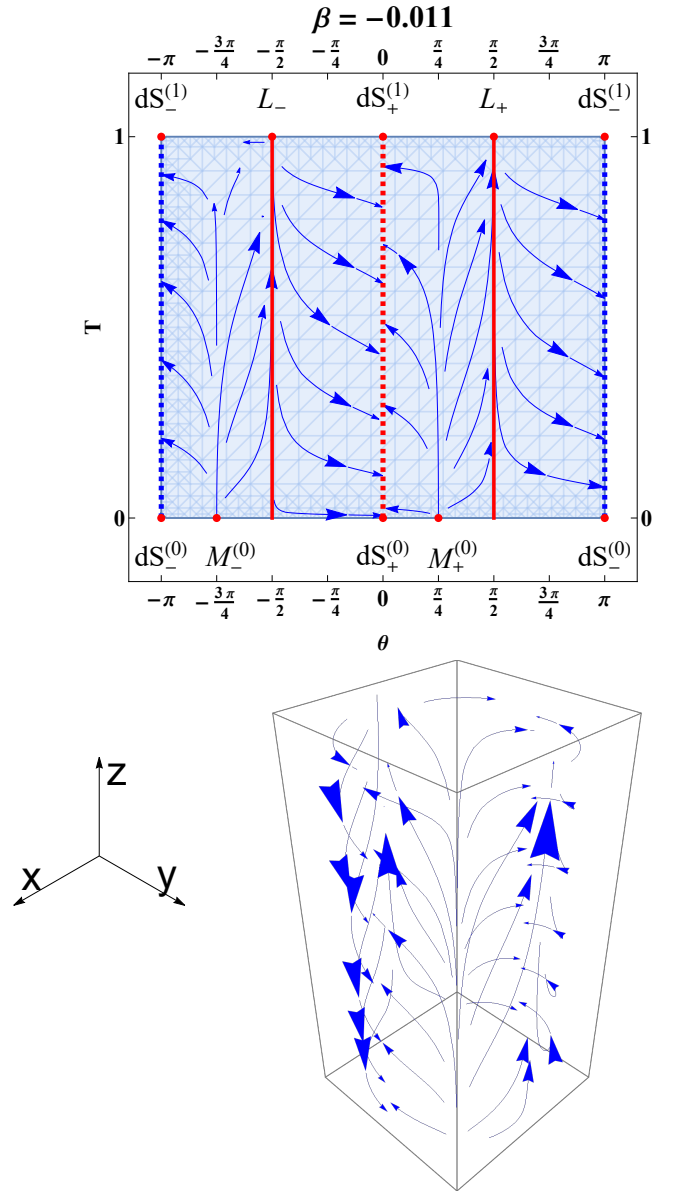


**Figure 4.** Phase-space plot of the dynamical system (58) and (59) of Kaniadakis horizon entropy cosmology with  $\Lambda \neq 0$ , for the best-fit value of Kaniadakis parameter obtained by the observational analysis, namely for  $\beta = -0.011$ . Upper panel: unwrapped solution space. Lower panel: projection over the cylinder  $\mathbf{S}$  defined in Cartesian coordinates  $(x, y, z)$  through (61). At late times the Universe results in a dark-energy dominated, de Sitter solution, while the past attractor is the matter-dominated epoch.

are the late-time de Sitter attractors. The early-time attractors are  $M_{\pm}^{(0)}$  for which  $q = 1/2$ , and they correspond to matter-dominated solutions. Hence, at late times the Universe results in a dark-energy dominated solution, while the past attractor of the Universe is the matter-dominated epoch. At the intersection of the invariant set  $T = 1$  with the singular lines  $\theta = \pm\pi/2$  we obtain the equilibrium points  $L_{\pm}$ . Considering that equations (58) and (59) diverge at  $L_{\pm}$ , we should introduce suitable variables for the analysis.

For the analysis at  $T = 1$  it proves convenient to define the variable

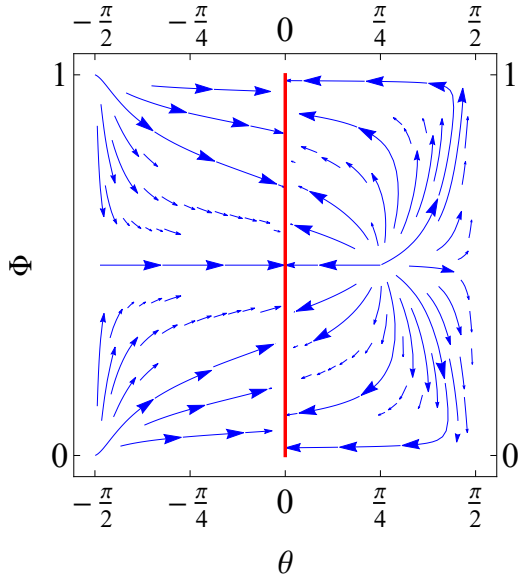


**Figure 5.** Phase-space plot of the system (64)-(65) of Kaniadakis horizon entropy cosmology with  $\Lambda \neq 0$ , for dust matter. The late attractor corresponds to  $\theta = 0$ , and thus to a dark-energy dominated solution with  $\Omega_{DE} = 1$ .

$$\Phi = \left\{ 1 + \exp \left[ \frac{|\beta|T^2}{(1-T)^2} \right] \right\}^{-1}, \quad \Phi \in [0, 1], \quad (62)$$

as well as the time rescaling

$$f' \equiv \frac{df}{d\zeta} = (1 - \Phi)^2 \frac{df}{d\eta} = \frac{\tanh^2 \left( \frac{\pi|K|}{2GH^2} \right) + 1}{4H} \dot{f}. \quad (63)$$

Hence, using also the variable  $\theta$  from (54), we finally obtain the autonomous system

$$\theta'(\zeta) = -\frac{3}{2} \sin(\theta) [2(\Phi - 1)\Phi(\sin(\theta) + \cos(\theta)) + \cos(\theta)], \quad (64)$$

$$\Phi'(\zeta) = 3(1 - \Phi)^2 \Phi^2 \tan(\theta) \ln [\Phi/(1 - \Phi)]. \quad (65)$$

In Fig. 5 we depict the phase-space flow of the system (64)-(65). Asymptotically,  $\theta \rightarrow 0$  and  $\Phi$  tends to a constant  $\Phi_0$ . Therefore, the late attractor corresponds to the dark-energy dominated solution with  $\Omega_{DE} = 1$ . The current values  $\Phi_0 = 1/(e^{|\beta|} + 1)$ ,  $\theta_0 = \arctan \left( \Omega_m^{(0)} \right)$  leads to the de Sitter solution  $a(t) = e^{H_0(t-t_0)}$ .

#### 4.1.1 Heteroclinic sequences

In the phase portrait of a dynamical system, a heteroclinic orbit is a path in phase space that joins two different equilibrium points. If the equilibrium points at the start and end of the orbit are the same, the orbit is a homoclinic orbit (Guckenheimer & Holmes 1983).

From the above analysis we can see that the invariant sets  $T = 0$  and  $T = 1$  are of interest in the determination of possible heteroclinic sequences. The direction of the flow can be determined by considering the monotonic function

$$M_1 = \frac{T}{1-T}, \quad M_1'(\tau) = \frac{3 \tan(\theta)}{2} M_1. \quad (66)$$

In if  $\tan(\theta) < 0$ , the orbits move from  $T = 1$  to  $T = 0$ , and if  $\tan(\theta) >$

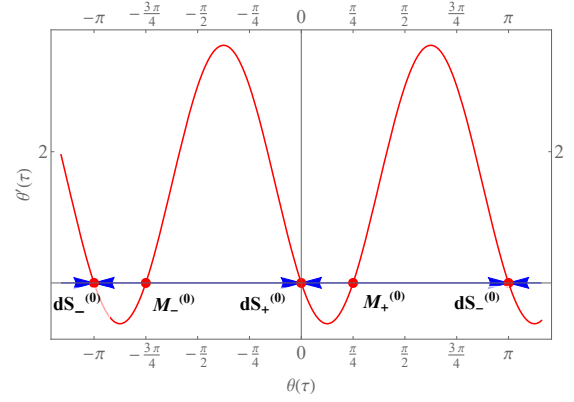


**Figure 6.** Phase-space diagram of the one-dimensional dynamical system (67) of Kaniadakis horizon entropy cosmology with  $\Lambda \neq 0$ , for dust matter and any value  $\beta$ .

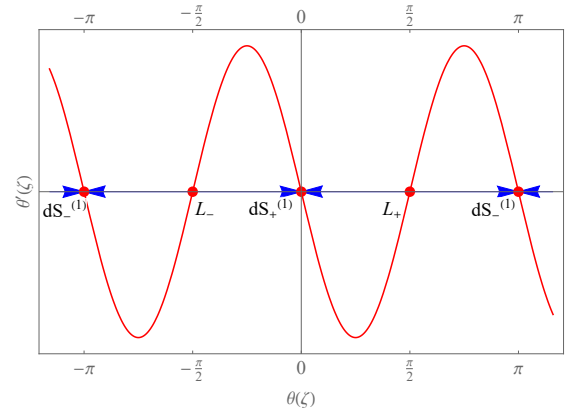


**Figure 7.** Phase-space diagram of the one-dimensional dynamical system (68) of Kaniadakis horizon entropy cosmology with  $\Lambda \neq 0$ , for dust matter and any value  $\beta$ .

0, the orbits move from  $T = 0$  to  $T = 1$ . In the invariant manifold  $T = 0$  ( $H \rightarrow \infty$ ) the dynamics is given by the one-dimensional flow

$$\theta'(\tau) = 3 \sin(\theta) (\sin(\theta) - \cos(\theta)). \quad (67)$$

In Fig. 6 we present the one-dimensional dynamical system (67), in which we can see the heteroclinic sequences  $M_+^{(0)} \rightarrow dS_+^{(0)}$  and  $M_-^{(0)} \rightarrow dS_-^{(0)}$ . Similarly, analyzing the one-dimensional flow in the invariant set  $T = 1$ , that corresponds to  $\Phi = 0$ , we find that the dynamics on this invariant set is given by the one-dimensional dynamical system

$$\theta'(\zeta) = -\frac{3}{2} \sin(\theta) \cos(\theta), \quad (68)$$

which has a behavior shown in Fig. 7, where the heteroclinic sequences  $L_+ \rightarrow dS_+^{(1)}$  and  $L_- \rightarrow dS_-^{(1)}$  are presented. Finally, to find heteroclinic sequences  $M_\pm^{(0)} \rightarrow dS_\pm^{(1)}$ , the intersection of the unstable manifold of  $M_\pm^{(0)}$  with the stable manifold of  $dS_\pm^{(1)}$  should be analyzed. Since the former is  $\mathbb{R}^2$ , then it is required to examine the stable manifold of  $dS_\pm^{(1)}$ . This is given locally by the graph

$$\left\{ (\Phi, \theta) \in \mathbb{R}^2 : \Phi = h(\theta), h(0) = 0, h'(0) = 0 \right\}, \quad |\theta| < \delta, \quad (69)$$

for  $\delta > 0$  suitably small. By the invariance of the stable manifold we

obtain the quasilinear differential equation for  $h$  given by

$$\frac{3}{2} \sin(\theta) h'(\theta) (2(h(\theta) - 1)h(\theta)(\sin(\theta) + \cos(\theta)) + \cos(\theta)) + 3(h(\theta) - 1)^2 h(\theta)^2 \tan(\theta) \ln\left(\frac{h(\theta)}{1-h(\theta)}\right) = 0. \quad (70)$$

Introducing the ansatz  $h(\theta) = a_1\theta^2 + a_2\theta^3 + a_3\theta^4 + \dots$ , we obtain  $a_i = 0$  at any order. Therefore, the dynamics at the stable manifold of  $dS_+^{(1)}$  is given by equation (68). Then, it is easy to construct heteroclinic sequences  $M_+^{(0)} \rightarrow dS_+^{(1)}$  which pass near the singularity  $L_+$  by assuming for instance the initial value  $(\Phi, \theta) = (\varepsilon, \pi/4)$ ,  $\varepsilon \approx 0$  and evolving the system back and forward in  $\zeta$ . Similar arguments can be used to construct heteroclinic sequences  $M_-^{(0)} \rightarrow dS_-^{(1)}$ , which pass near the singularity  $L_-$ , with the initial value  $(\Phi, \theta) = (\varepsilon, -3\pi/4)$ ,  $\varepsilon \approx 0$ .

Summarizing, for  $0 \leq \theta \leq \pi/2$  (the physical region is  $0 \leq \theta \leq \pi/4$ ), there exists the heteroclinic sequences  $M_+^{(0)} (\Omega_m \rightarrow 1, H \rightarrow \infty) \rightarrow L_+ (\Omega_m \rightarrow +\infty, H \rightarrow 0) \rightarrow dS_+^{(1)}$  (de Sitter,  $\Omega_m \rightarrow 0, H \rightarrow 0$ ) and  $M_+^{(0)} \rightarrow dS_+^{(0)}$  (de Sitter,  $\Omega_m \rightarrow 0, H \rightarrow \infty$ ), and in the region  $-\pi \leq \theta \leq -\pi/2$  (the physical region is  $-\pi \leq \theta \leq -3\pi/4$ ), there exists the heteroclinic sequences  $M_-^{(0)} (\Omega_m \rightarrow 1, H \rightarrow \infty) \rightarrow L_- (\Omega_m \rightarrow -\infty, H \rightarrow 0) \rightarrow dS_-^{(1)}$  (de Sitter,  $\Omega_m \rightarrow 0, H \rightarrow 0$ ) and  $M_-^{(0)} \rightarrow dS_-^{(0)}$  (de Sitter,  $\Omega_m \rightarrow 0, H \rightarrow \infty$ ).

#### 4.1.2 Bounce and a turnaround

Another interesting cosmological possibility is the possible existence of a bounce and a turnaround (Saridakis 2009; Cai et al. 2012; Zhu et al. 2021). Let us assume that, for the state vector  $(a, H, R)$ , the field equations can be written as

$$\dot{a} = aH, \quad (71)$$

$$\dot{H} = \frac{1}{6} (R - 12H^2), \quad (72)$$

$$\dot{R} = g(a, H, R), \quad (73)$$

such that the function  $g(a, H, R)$  satisfies  $g(a, H, R) = -g(a, -H, R)$ . Hence, the system (71), (72) and (73) is invariant under time inversion  $t \mapsto -t$  if also  $H \mapsto -H$  and  $R \mapsto R$ , and by definition  $a \geq 0$ . Those solutions can be related to symmetric cyclic solutions with respect to the origin, chosen to correspond to the possible bounce point  $t_{\text{bounce}} = 0$ . Therefore, if the bounce exists, the system (71), (72) and (73) is a reversible system in the sense that it has a reversing symmetry under time inversion.

Let us consider the simplest case where there is exactly one bouncing and exactly one turnaround point. Note that both at the bounce and turnaround points we have  $H = 0$ . In this case, the line connecting these points and corresponding to  $H = 0$  defines a plane that separates all points on the trajectory in this phase space to the ones corresponding to either the expanding ( $H > 0$ ) or contracting ( $H < 0$ ) phase. As discussed in Pavlović & Sossich (2021), it is natural that in cyclic models the value of the Ricci scalar would approach its maximum around the bounce and since  $\dot{H} > 0$ , from (72) it follows that this maximum Ricci scalar value is positive, and moreover that  $\ddot{H} = 0$  at the bounce.

In summary, at the bounce we have  $R = R_{\text{bounce}} > 0$ ,  $H = 0$ , and  $a = a_{\text{min}}$ . The bounce is then followed by a phase in which  $\dot{H} > 0$ ,  $H > 0$ ,  $\dot{a} > 0$ , and  $\dot{R} < 0$ . Then the Universe enters the phase characterized by  $\dot{H} < 0$  and approaches the turnaround point which is determined by  $H = 0$ ,  $a = a_{\text{max}}$ , and  $R = R_{\text{turnaround}} < 0$ , where the last condition follows from Eq. (72).

To obtain  $g(a, H, R)$  in Eq. (73), we use Eqs. (8), (9), (11), (12), and (14), where for simplicity we focus on the dust case. Therefore, we obtain

$$\begin{aligned} R &= 6\dot{H} + 12H^2 = -24\pi G\rho_{DE} \\ &= 3 \left\{ -8\pi G\rho_m \left[ \operatorname{sech}\left(\frac{\beta H_0^2}{H^2}\right) - 1 \right] \right. \\ &\quad \left. + 3\beta H_0^2 \operatorname{shi}\left(\frac{H_0^2\beta}{H^2}\right) - 3H^2 \left[ \cosh\left(\frac{\beta H_0^2}{H^2}\right) - 1 \right] + \Lambda \right\}. \end{aligned} \quad (74)$$

Introducing the dimensionless quantities  $E = \frac{H}{H_0}$  and  $\mathcal{R} = \frac{R}{12H_0^2}$ , and using  $z$  as the independent variable, we extract the general system for  $(a, E, \mathcal{R})$ :

$$\frac{da}{dz} = -a^2, \quad (75)$$

$$\frac{dE}{dz} = -2 \left( \mathcal{R} - E^2 \right) \frac{a}{E}, \quad (76)$$

$$\frac{d\mathcal{R}}{dz} = - \frac{9\beta\Omega_m^{(0)2} \tanh\left(\frac{\beta}{E^2}\right) \operatorname{sech}^2\left(\frac{\beta}{E^2}\right)}{4E^4 a^5}. \quad (77)$$

Finally, in order to examine whether the above requirements are fulfilled in the present scenario, we use the best fit values  $\beta = -0.011$  and  $\Omega_m^{(0)} = 0.283$  in (75), (76) and (77), and we find

$$\frac{da}{dz} = -a^2, \quad (78)$$

$$\frac{dE}{dz} = -2 \left( \mathcal{R} - E^2 \right) \frac{a}{E}, \quad (79)$$

$$\frac{d\mathcal{R}}{dz} = - \frac{0.0019822 \tanh\left(\frac{0.011}{E^2}\right) \operatorname{sech}^2\left(\frac{0.011}{E^2}\right)}{E^4 a^5}. \quad (80)$$

In the case of dust matter and  $\Lambda \neq 0$ . This system cannot satisfy the above requirements, and hence the present scenario cannot exhibit bounce and turnaround solutions.

#### 4.2 Case II: $\Lambda = 0$

In the case  $\Lambda = 0$ , eq. (10) becomes

$$\frac{8\pi G\rho_m}{3H^2} = - \frac{3\pi K \operatorname{shi}\left(\frac{K\pi}{GH^2}\right)}{3GH^2} + \cosh\left(\frac{\pi K}{GH^2}\right). \quad (81)$$

This expression is used as a definition of  $\rho_m$ . If  $\beta \neq 0$ , and re-scaling the time derivative  $d/dv = (1-T)d/d\tau$ , we obtain

$$T'(v) = \frac{3}{2} (1-T)^2 T \cosh\left(\frac{\beta T^2}{(1-T)^2}\right) - \frac{3}{2} \beta T^3 \operatorname{shi}\left(\frac{T^2\beta}{(1-T)^2}\right). \quad (82)$$

The equilibrium points of (82) are  $T = 0$ , which is unstable, and the equilibrium point  $T = T_c$ , where  $T_c$  is a solution of the transcendental equation  $(1-T_c)^2 \cosh\left(\beta T_c^2/(1-T_c)^2\right) - \beta T_c^3 \operatorname{shi}\left(T_c^2\beta/(1-T_c)^2\right) = 0$ ,

$0 < T_c < 1$ , corresponding to de Sitter solution  $a(t) \propto e^{H_0 t \left(\frac{1}{T_c} - 1\right)}$ , is stable. In Fig. 8 we depict a phase-space plot of the one-dimensional dynamical system (82) of Kaniadakis horizon entropy cosmology with  $\Lambda = 0$ , for dust matter, and the join value  $\beta = 1.161$ . Note that all orbits originate from the invariant subset  $T = 0$ , classically related to the initial singularity with  $H \rightarrow \infty$ . The late-time attractor is  $T = T_c \approx 0.521$ , and it corresponds to de Sitter solution.

Finally, in order to examine whether the present scenario exhibits a bounce, we use the best fit values  $\beta = 1.161$  and  $\Omega_m^{(0)} = 0.326$  in

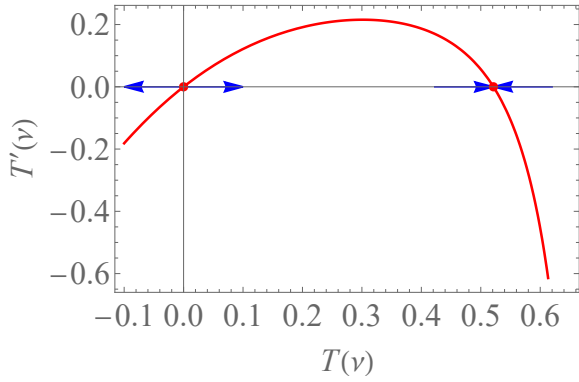


**Figure 8.** Phase-space diagram of the one-dimensional dynamical system (82) of Kaniadakis horizon entropy cosmology with  $\Lambda = 0$ , for dust matter and for the best-fit value of Kaniadakis parameter obtained by the observational analysis, namely for  $\beta = 1.161$ . The physical region is  $0 \leq T < 1$ . The equilibrium point  $T = 0$  is unstable, dominated by dark-energy, and de Sitter equilibrium point  $T = T_c \approx 0.521$  is stable.

(75), (76) and (77) and we find

$$\frac{da}{dz} = -a^2, \quad (83)$$

$$\frac{dE}{dz} = -2 \left( \mathcal{R} - E^2 \right) \frac{a}{E}, \quad (84)$$

$$\frac{d\mathcal{R}}{dz} = \frac{0.277619 \tanh\left(\frac{1.161}{E^2}\right) \operatorname{sech}^2\left(\frac{1.161}{E^2}\right)}{E^4 a^5}, \quad (85)$$

in the case of dust matter and  $\Lambda = 0$ , we deduce that the system cannot fulfill the bounce requirements, and therefore it cannot exhibit bounce and turnaround solutions.

## 5 SUMMARY AND DISCUSSION

The present work was devoted to explore Kaniadakis horizon entropy cosmology which arises from the application of the gravity-thermodynamics conjecture using the Kaniadakis modified entropy. The resulting modified Friedmann equations contain extra terms that constitute an effective dark energy sector. Moreover, we used data from Observational Hubble Data, Supernova Type Ia, HII galaxies, Strong Lensing Systems, and Baryon Acoustic Oscillations observations, and we applied a Bayesian Markov Chain Monte Carlo analysis in order to construct the likelihood contours for the model parameters.

Regarding the Kaniadakis parameter  $\beta$ , we found that it is constrained around 0, namely around the value in which standard Bekenstein-Hawking is recovered. Furthermore, the present matter density parameter  $\Omega_m^{(0)}$  is consistent with the expected value from  $\Lambda$ CDM scenario, having a lower value for the  $\Lambda \neq 0$  case and a slightly higher value for the  $\Lambda = 0$  case.

However, the interesting result comes from the constraint on the normalized Hubble parameter  $h$ . In particular, for  $\Lambda \neq 0$  we extracted  $h = 0.708^{+0.012}_{-0.011}$  while for  $\Lambda = 0$  we found  $h = 0.715^{+0.012}_{-0.012}$ . Thus, the obtained value of  $H_0$  for  $\Lambda \neq 0$  deviates  $2.67\sigma$  from the Planck value and  $1.74\sigma$  from the SH0ES one, while in the  $\Lambda = 0$  case the deviation is  $3\sigma$  from the Planck value and  $1.36\sigma$  from the SH0ES one. Additionally, in order to verify this result in an independent way, we performed the  $H_0(z)$  diagnostic. Hence, our analysis reveals that Kaniadakis horizon entropy cosmology is an interesting candidate to alleviate the  $H_0$  tension problem. This is one of the main results of the present work.

We proceeded by investigating the cosmographic parameters, namely the deceleration and jerk ones, by using the data in order to reconstruct them in the redshift region  $0 < z < 2.5$ . As we showed, the transition from deceleration to acceleration happens at  $z_T = 0.715^{+0.042}_{-0.041}$  for the  $\Lambda \neq 0$  case and at  $z_T = 0.652^{+0.032}_{-0.031}$  for the  $\Lambda = 0$  case, in agreement within  $1\sigma$  with that found in Herrera-Zamorano et al. (2020) for  $\Lambda$ CDM cosmology. Furthermore, we applied the AICc and BIC information criteria and we found that although AICc suggests that  $\Lambda \neq 0$  model and  $\Lambda$ CDM are statistically equivalent in the joint analysis, BIC indicates that there is a strong evidence against the candidate model. Lastly, applying the DIC criterion we found that the  $\Lambda \neq 0$  case and  $\Lambda$ CDM are statistical equivalent for BAO, they have a moderate tension for OHD and SLS, and a strong tension for HIIG and SNIa datasets, while the  $\Lambda \neq 0$  case and  $\Lambda$ CDM are statistical equivalent for all datasets.

Finally, we performed a detailed dynamical-system analysis, providing a general description of the phase-space of all possible solutions of the system, their equilibrium points and stability, as well as the late-time asymptotic behavior. As we showed, the Universe past attractor is the matter-dominated epoch, while at late times the Universe results in the dark-energy-dominated solution, for both  $\Lambda = 0$ , and  $\Lambda \neq 0$  cases. Moreover, we showed that the scenario accepts heteroclinic sequences, but it cannot lead to bounce and turnaround solutions.

In summary, the scenario of Kaniadakis horizon entropy cosmology exhibits very interesting phenomenology and is in agreement with observational behavior. Hence, it can be an interesting candidate for the description of Nature.

## ACKNOWLEDGMENTS

We thank the anonymous referee for thoughtful remarks and suggestions. A.H.A. thanks to the PRODEP project, Mexico for resources and financial support and thanks also to the support from Luis Aguilar, Alejandro de León, Carlos Flores, and Jair García of the Laboratorio Nacional de Visualización Científica Avanzada. G.L. was funded by Agencia Nacional de Investigación y Desarrollo - ANID for financial support through the program FONDECYT Iniciación grant no. 11180126 and by Vicerrectoría de Investigación y Desarrollo Tecnológico at UCN. J.M. acknowledges the support from ANID project Basal AFB-170002 and ANID REDES 190147. M.A.G.-A. acknowledges support from Universidad Iberoamericana that support with the SNI grant, ANID REDES (190147), Cátedra Marcos Moshinsky and Instituto Avanzado de Cosmología (IAC). V.M. acknowledges support from Centro de Astrofísica de Valparaíso and ANID REDES 190147. This work is partially supported by the Ministry of Education and Science of the Republic of Kazakhstan, Grant AP08856912. A.D. Millano was supported by Agencia Nacional de Investigación y Desarrollo - ANID-Subdirección de Capital Humano/Doctorado Nacional/año 2020- folio 21200837 and by Vicerrectoría de Investigación y Desarrollo Tecnológico at UCN.

## DATA AVAILABILITY

The data underlying this article were cited in Section 3.1.

## REFERENCES

Abreu E. M. C., Ananias Neto J., 2021, *EPL*, 133, 49001



- Abreu E. M. C., Ananias Neto J., Barboza E. M., Nunes R. C., 2016, *EPL*, 114, 55001
- Abreu E. M. C., Neto J. A., Mendes A. C. R., Bonilla A., 2018, *EPL*, 121, 45002
- Addazi A., et al., 2021 ([arXiv:2111.05659](https://arxiv.org/abs/2111.05659))
- Aghanim N., et al., 2020, *Astron. Astrophys.*, 641, A6
- Akaike H., 1974, *IEEE Transactions on Automatic Control*, 19, 716
- Akbar M., Cai R.-G., 2006, *Phys. Lett. B*, 635, 7
- Akbar M., Cai R.-G., 2007, *Phys. Rev. D*, 75, 084003
- Amante M. H., Magaña J., Motta V., García-Aspeitia M. A., Verdugo T., 2020, *MNRAS*, 498, 6013–6033
- Asimakis P., Basilakos S., Mavromatos N. E., Saridakis E. N., 2021, Big Bang Nucleosynthesis constraints on higher-order modified gravities ([arXiv:2112.10863](https://arxiv.org/abs/2112.10863))
- Bak D., Rey S.-J., 2000, 2007, *Class. Quant. Grav.*, 17, L83
- Barrow J. D., 2020, *Phys. Lett. B*, 808, 135643
- Barrow J. D., Basilakos S., Saridakis E. N., 2021a, *Phys. Lett. B*, 815, 136134
- Barrow J. D., Basilakos S., Saridakis E. N., 2021b, *Physics Letters B*, 815, 136134
- Beutler F., et al., 2011, *MNRAS*, 416, 3017
- Blake C., et al., 2011, *MNRAS*, 418, 1707
- Cai R.-G., Cao L.-M., 2007, *Phys. Rev. D*, 75, 064008
- Cai R.-G., Kim S. P., 2005, *JHEP*, 02, 050
- Cai R.-G., Ohta N., 2010, *Phys. Rev. D*, 81, 084061
- Cai R.-G., Cao L.-M., Hu Y.-P., 2009, *Class. Quant. Grav.*, 26, 155018
- Cai Y.-F., Gao C., Saridakis E. N., 2012, *JCAP*, 10, 048
- Capozziello S., Lambiase G., Saridakis E. N., 2017, *Eur. Phys. J. C*, 77, 576
- Carroll S. M., 2001, *Living Rev. Rel.*, 4, 1
- Chen X.-m., Gong Y.-g., Saridakis E. N., 2009, *JCAP*, 0904, 001
- Chen L., Huang Q.-G., Wang K., 2019, *J. Cosmology Astropart. Phys.*, 2019, 028
- Coley A. A., 2003, *Dynamical systems and cosmology*. Vol. 291, Kluwer, Dordrecht, Netherlands, [doi:10.1007/978-94-017-0327-7](https://doi.org/10.1007/978-94-017-0327-7)
- Copeland E. J., Liddle A. R., Wands D., 1998, *Phys. Rev.*, D57, 4686
- Copland E. J., Sami M., Tsujikawa S., 2006, *Int. J. Mod. Phys.*, D15, 1753
- Cotsakis S., Kittou G., 2013, *Phys. Rev.*, D88, 083514
- Drepanou N., Lympers A., Saridakis E. N., Yesmakhanova K., 2021 ([arXiv:2109.09181](https://arxiv.org/abs/2109.09181))
- Fan Z.-Y., Lu H., 2015, *Phys. Rev. D*, 91, 064009
- Ferreira P. G., Joyce M., 1997, *Phys. Rev. Lett.*, 79, 4740
- Foreman-Mackey D., Hogg D. W., Lang D., Goodman J., 2013, *PASP*, 125, 306
- Frolov A. V., Kofman L., 2003, *JCAP*, 05, 009
- García-Aspeitia M. A., Hernández-Almada A., 2021, *Phys. Dark Univ.*, 32, 100799
- García-Aspeitia M. A., Hernandez-Almada A., Magaña J., Amante M. H., Motta V., Martínez-Robles C., 2018, *Phys. Rev. D*, 97, 101301
- García-Aspeitia M. A., Martínez-Robles C., Hernández-Almada A., Magaña J., Motta V., 2019, *Phys. Rev.*, D99, 123525
- García-Aspeitia M. A., Hernández-Almada A., Magaña J., Motta V., 2021, *Phys. Dark Univ.*, 32, 100840
- Giambo R., Miritzis J., 2010, *Class. Quant. Grav.*, 27, 095003
- Gibbons G. W., Hawking S. W., 1977, *Phys. Rev. D*, 15, 2738
- Gim Y., Kim W., Yi S.-H., 2014, *JHEP*, 07, 002
- Giostrì R., dos Santos M. V., Waga I., Reis R., Calvão M., Lago B. L., 2012, *Journal of Cosmology and Astroparticle Physics*, 2012, 027
- González-Morán A. L., et al., 2021, *MNRAS*, 505, 1441
- Guckenheimer J., Holmes P., 1983, *Nonlinear Oscillations, Dynamical Systems, and Bifurcations of Vector Fields*. (Applied Mathematical Sciences Vol. 42), Springer
- Hernández-Almada, A. Magaña, Juan García-Aspeitia, Miguel A. Motta, V. 2019, *Eur. Phys. J. C*, 79, 12
- Hernández-Almada A., Leon G., Magaña J., García-Aspeitia M. A., Motta V., Saridakis E. N., Yesmakhanova K., 2022, *Monthly Notices of the Royal Astronomical Society*, 511, 4147–4158
- Herrera-Zamorano L., Hernández-Almada A., García-Aspeitia M. A., 2020, *Eur. Phys. J. C*, 80, 637
- Hurvich C. M., Tsai C. L., 1989, *Biometrika*, 76, 297
- Jacobson T., 1995, *Phys. Rev. Lett.*, 75, 1260
- Jamil M., Saridakis E. N., Setare M. R., 2010a, *JCAP*, 11, 032
- Jamil M., Saridakis E. N., Setare M. R., 2010b, *Phys. Rev. D*, 81, 023007
- Jeffreys H., 1961, *Theory of Probability*, third edn. Oxford, Oxford, England
- Kaniadakis G., 2002, *Phys. Rev. E*, 66, 056125
- Kaniadakis G., 2005, *Phys. Rev. E*, 72, 036108
- Krishnan C., Ó Colgáin E., Sheikh-Jabbari M., Yang T., 2021, *Phys. Rev. D*, 103, 023503
- Kunz M., Trotta R., Parkinson D. R., 2006, *Phys. Rev. D*, 74, 023503
- Leon G., Magaña J., Hernández-Almada A., García-Aspeitia M. A., Verdugo T., Motta V., 2021, *JCAP*, 12, 032
- Liddle A., 2007, *MNRAS: Letters*, 377
- Lympers A., Saridakis E. N., 2018, *Eur. Phys. J. C*, 78, 993
- Lympers A., Basilakos S., Saridakis E. N., 2021, *Eur. Phys. J. C*, 81, 1037
- Lyra M. L., Tsallis C., 1998, *Phys. Rev. Lett.*, 80, 53
- Moradpour H., Ziaie A. H., Kord Zangeneh M., 2020, *Eur. Phys. J. C*, 80, 732
- Moresco M., et al., 2016, *JCAP*, 1605, 014
- Motta V., García-Aspeitia M. A., Hernández-Almada A., Magaña J., Verdugo T., 2021, *Universe*, 7, 163
- Nadathur S., Percival W. J., Beutler F., Winther H., 2020, *Phys. Rev. Lett.*, 124, 221301
- Padmanabhan T., 2005, *Phys. Rept.*, 406, 49
- Padmanabhan T., 2010, *Rept. Prog. Phys.*, 73, 046901
- Papagiannopoulos G., Basilakos S., Saridakis E. N., 2022, Dynamical system analysis of Myrzakulov gravity ([arXiv:2202.10871](https://arxiv.org/abs/2202.10871))
- Paranjape A., Sarkar S., Padmanabhan T., 2006, *Phys. Rev. D*, 74, 104015
- Pavlović P., Sossich M., 2021, *Phys. Rev. D*, 103, 023529
- Percival W. J., et al., 2010, *MNRAS*, 401, 2148
- Perko L., 2000, *Differential Equations and Dynamical Systems*, Third Edition. Springer
- Pospelov M., Pradler J., 2010, *Annual Review of Nuclear and Particle Science*, 60, 539
- Riess A. G., Filippenko A. V., Challis P., Clocchiatti A., Diercks A., et al., 1998, *The Astronomical Journal*, 116, 1009
- Riess A. G., Casertano S., Yuan W., Macri L. M., Scolnic D., 2019, *The Astrophysical Journal*, 876, 85
- Riess A. G., Casertano S., Yuan W., Bowers J. B., Macri L., Zinn J. C., Scolnic D., 2021, *Astrophys. J. Lett.*, 908, L6
- Saridakis E. N., 2009, *Nucl. Phys. B*, 808, 224
- Saridakis E. N., 2020, *JCAP*, 07, 031
- Saridakis E. N., Basilakos S., 2021, *Eur. Phys. J. C*, 81, 7
- Saridakis E. N., et al., 2021 ([arXiv:2105.12582](https://arxiv.org/abs/2105.12582))
- Schwarz G., 1978, *Ann. Statist.*, 6, 461
- Scolnic D. M., et al., 2018, *Astrophys. J.*, 859, 101
- Sheykhi A., 2010a, *Eur. Phys. J. C*, 69, 265
- Sheykhi A., 2010b, *Phys. Rev. D*, 81, 104011
- Sheykhi A., 2018, *Phys. Lett. B*, 785, 118
- Sheykhi A., Wang B., Cai R.-G., 2007, *Nucl. Phys. B*, 779, 1
- Spergel D. N., et al., 2003, *Astrophys. J. Suppl.*, 148, 175
- Spiegelhalter D. J., Best N. G., Carlin B. P., Van Der Linde A., 2002, *Journal of the Royal Statistical Society: Series B (Statistical Methodology)*, 64, 583
- Sugiura N., 1978, *Communications in Statistics - Theory and Methods*, 7, 13
- Tsallis C., 1988, *Journal of Statistical Physics*, 52, 479
- Wainwright J., Ellis G. F. R., 1997, *Dynamical Systems in Cosmology*. Cambridge University Press
- Wang M., Jing J., Ding C., Chen S., 2010, *Phys. Rev. D*, 81, 083006
- Weinberg S., 1989, *Rev. Mod. Phys.*, 61, 1
- Zel'dovich Y., Krasinski A., Zeldovich Y., 1968, *Sov. Phys. Usp.*, 11, 381
- Zhu M., Ilyas A., Zheng Y., Cai Y.-F., Saridakis E. N., 2021, *JCAP*, 11, 045

This paper has been typeset from a  $\text{\TeX}/\text{\LaTeX}$  file prepared by the author.